Functional and Structural Role of Amino Acid Residues in the Even-numbered Transmembrane α-Helices of the Bovine Mitochondrial Oxoglutarate Carrier

ARTICLE *in* JOURNAL OF MOLECULAR BIOLOGY · NOVEMBER 2006

Impact Factor: 4.33 · DOI: 10.1016/j.jmb.2006.08.041 · Source: PubMed

doi:10.1016/j.jmb.2006.08.041 J. Mol. Biol. (2006) 363, 51–62

JMB

Available online at www.sciencedirect.com

ScienceDirect

ELSEVIER

Functional and Structural Role of Amino Acid Residues in the Even-numbered Transmembrane α-Helices of the Bovine Mitochondrial Oxoglutarate Carrier

Anna Rita Cappello[1,2], Rosita Curcio[1], Daniela Valeria Miniero[1] Italo Stipani[1,3], Alan J. Robinson[4], Edmund R. S. Kunji[4]* and Ferdinando Palmieri[1,3]*

[1]*Department of Pharmaco-Biology, Laboratory of Biochemistry and Molecular Biology, University of Bari Via E. Orabona 4 70125 Bari, Italy*

[2]*Department of Pharmaco-Biology, University of Calabria, Via P. Bucci 87036 Cosenza, Italy*

[3]*CNR Institute of Biomembranes and Bioenergetics, Via E. Orabona 4 70125 Bari, Italy*

[4]*The Medical Research Council Dunn Human Nutrition Unit Hills Road, CB2 2XY Cambridge, United Kingdom*

**Corresponding authors*

The mitochondrial oxoglutarate carrier exchanges cytosolic malate for 2-oxoglutarate from the mitochondrial matrix. Orthologs of the carrier have a high degree of amino acid sequence conservation, meaning that it is impossible to identify residues important for function on the basis of this criterion alone. Therefore, each amino acid residue in the transmembrane α-helices H2 and H6 was replaced by a cysteine in a functional mitochondrial oxoglutarate carrier that was otherwise devoid of cysteine residues. The effects of the cysteine replacement and subsequent modification by sulfhydryl reagents on the initial uptake rate of 2-oxoglutarate were determined. The results were evaluated using a structural model of the oxoglutarate carrier. Residues involved in inter-helical and lipid bilayer interactions tolerate cysteine replacements or their modifications with little effect on transport activity. In contrast, the majority of cysteine substitutions in the aqueous cavity had a severe effect on transport activity. Residues important for function of the carrier cluster in three regions of the transporter. The first consists of residues in the [YWLF]- [KR]-G-X-X-P sequence motif, which is highly conserved in all members of the mitochondrial carrier family. The residues may fulfill a structural role as a helix breaker or a dynamic role as a hinge region for conformational changes during translocation. The second cluster of important residues can be found at the carboxy-terminal end of the even-numbered transmembrane α-helices at the cytoplasmic side of the carrier. Residues in H6 at the interface with H1 are the most sensitive to mutation and modification, and may be essential for folding of the carrier during biogenesis. The third cluster is at the midpoint of the membrane and consists of residues that are proposed to be involved in substrate binding.

Keywords: cysteine scanning mutagenesis; membrane transport proteins; mitochondria; oxoglutarate carrier; structural modeling

Introduction

The mitochondrial oxoglutarate carrier (OGC) catalyzes the transport of 2-oxoglutarate across the mitochondrial inner membrane in exchange for malate, or other dicarboxylates, and plays an important role in several metabolic processes.[1] The carrier is an essential component of the malate/aspartate shuttle that effectively transfers reducing equivalents from cytosolic NADH to NAD^+ in the mitochondrial matrix of eukaryotic

Abbreviations used: MTSES, sodium(2-sulfonatoethyl)-methanethiosulfonate; MTSET, [2-(trimethylammonium) ethyl]methanethiosulfonate bromide; OGC, oxoglutarate carrier; C-less OGC, cysteine-less OGC; PCR, polymerase chain reaction.

E-mail addresses of the corresponding authors: ek@mrc-dunn.cam.ac.uk; fpalm@farmbiol.uniba.it

0022-2836/$ - see front matter

cells. Furthermore, the OGC participates in the oxoglutarate/isocitrate shuttle, in gluconeogenesis from lactate and in nitrogen metabolism. The OGC belongs to a large family of related transport proteins called the mitochondrial transporter family.[2] The primary structures of the family members are made up of three tandemly repeated homologous domains of about 100 amino acids in length. A characteristic amino acid sequence motif P-X- [DE]-X-X- [RK] is present in all members of the family and in all three repeats (PROSITE PS50920 and PFAM PF00153). The atomic model of the bovine mitochondrial ADP/ATP carrier 1 (AAC1), which is a member of the protein family, has clarified the structural role of these sequence features.[3] The main structural fold is a six α-helical bundle with 3-fold pseudo-symmetry.[3,4] The proline residues of the signature motif induce sharp kinks in the odd-numbered α-helices, closing the central pore of the α-helical bundle at the matrix side. These α-helices are held together by salt bridges that are formed between the charged residues of the three signature motifs,[3] as predicted by an analysis of second-site revertants.[5] The significant sequence conservation in the mitochondrial carrier family suggests that the main structural fold is similar for all carriers and that the specific recognition of substrates is coupled to a common structural mechanism of transport. Based on comparative modeling, a common substrate binding site was proposed by considering distance and chemical constraints, and the conservation of amino acids.[6] The proposed binding site explains substrate selectivity, ion coupling and the effects of the membrane potential on transport. However, the structural changes that are required for the translocation of the substrate are unknown.

Here, cysteine scanning mutagenesis was applied to probe the structure of OGC and to establish the functionally important residues of the transmembrane α-helices H2 and H6. The results were combined with those obtained for transmembrane α-helix H4.[7] As there is no structure available for the OGC, the results are interpreted in the context of a comparative model of OGC based on the structure of the bovine AAC1.[3] In addition, labeling studies with cysteine-reactive reagents sodium(2-sulfonatoethyl)-methanethiosulfonate (MTSES) and [2-(trimethylammonium)ethyl] methanethiosulfonate bromide (MTSET) were carried out to establish accessibility and whether positions in the carrier can tolerate a large substitution. These studies have highlighted amino acid positions that are critical for the function of the carrier.

Results

Transport activity of reconstituted OGC mutants

The subfamily of mitochondrial oxoglutarate carriers are known to be present in plants, worms, insects, fish, amphibians, and mammals. The amino acid sequence conservation of the even-numbered transmembrane α-helices of OGC is higher than that of the odd-numbered transmembrane α-helices. The percentage of strictly conserved amino acid residues is 52%, 63% and 79% for α-helices H2, H4 and H6, whereas it is 50%, 32% and 42% for α-helices H1, H3 and H5, respectively. The cavity of the OGC contains the largest number of conserved amino acid residues whereas the residues that interact with the lipid bilayer are often substituted by other hydrophobic residues (Figure 1). Since conservation alone cannot be used to identify functionally important residues, cysteine scanning mutagenesis was applied. By using a functional cysteine-less OGC, each amino acid residue in transmembrane H2 and H6 was replaced by a cysteine. The expression levels of the mutant OGC, overproduced in *Escherichia coli*, ranged between 54% and 120% as compared to those of the wild-type OGC, except for Q91C and S277C, which did not express (data not shown). The recombinant proteins were refolded and reconstituted into liposomes to measure transport rates of 2-oxoglutarate. The amount of reconstituted wild-type and mutant proteins varied between 16% and 32% of the added protein, which is similar to values found for other recombinant reconstituted mitochondrial carrier proteins.[7–14] For transmembrane α-helices H2 and H6, Figure 2 shows the initial transport rates of 2-oxoglutarate for each recombinant OGC as a percentage of the cysteine-less value. The effects of the mutations on the initial transport rate were mapped on the comparative model of OGC (Figure 3) together with the published data for H4.[7] The mutations that virtually abolished transport were Y81C, G83C, G87C, R90C, Y94C, R98C, L99C, G100C and Y102C in H2 and R288C, T293C, F297C, E301C, M303C, and N304C in H6 (Figures 2 and 3). To exclude the possibility that the transport properties were due to a combination of mutations, the same mutations were cloned in the wild-type gene. With the exception of M303C and N304C, the resulting mutant carriers were also unable to transport 2-oxoglutarate, demonstrating that the majority of the single mutations abolish transport (Figure 4). The essential residues G83, G87, R90, Y94, R98 in H2 and R288, T293, F297, and E301 in H6 were mutated into a range of other residues in the

Figure 1. Conservation of amino acid residues in oxoglutarate carriers. The structural model of bovine OGC is shown in cartoon (a) and surface representation (b) with a view into the cavity from the cytoplasmic side (first panel) and lateral views from opposite sides (second and third panel). Amino acid positions that are strictly conserved within the set of oxoglutarate carriers are colored orange, those that have two or three amino acid substitutions yellow and those with four and more substitutions green. The loop regions, matrix α-helices and the odd-numbered α-helices are colored in wheat. The strictly conserved residues are also labeled with their one-letter amino acid code and their position.

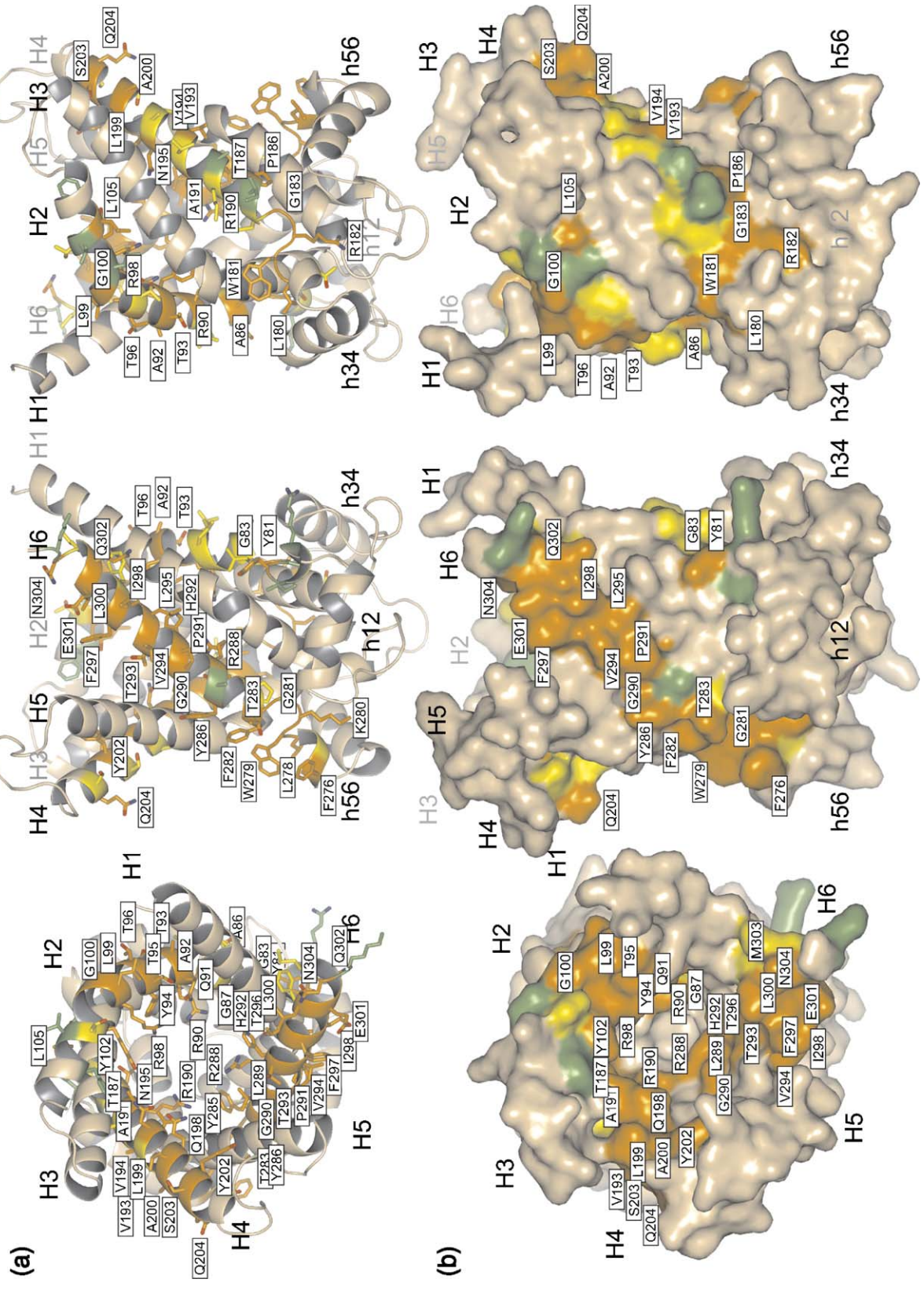

Figure 1 (*legend on previous page*)

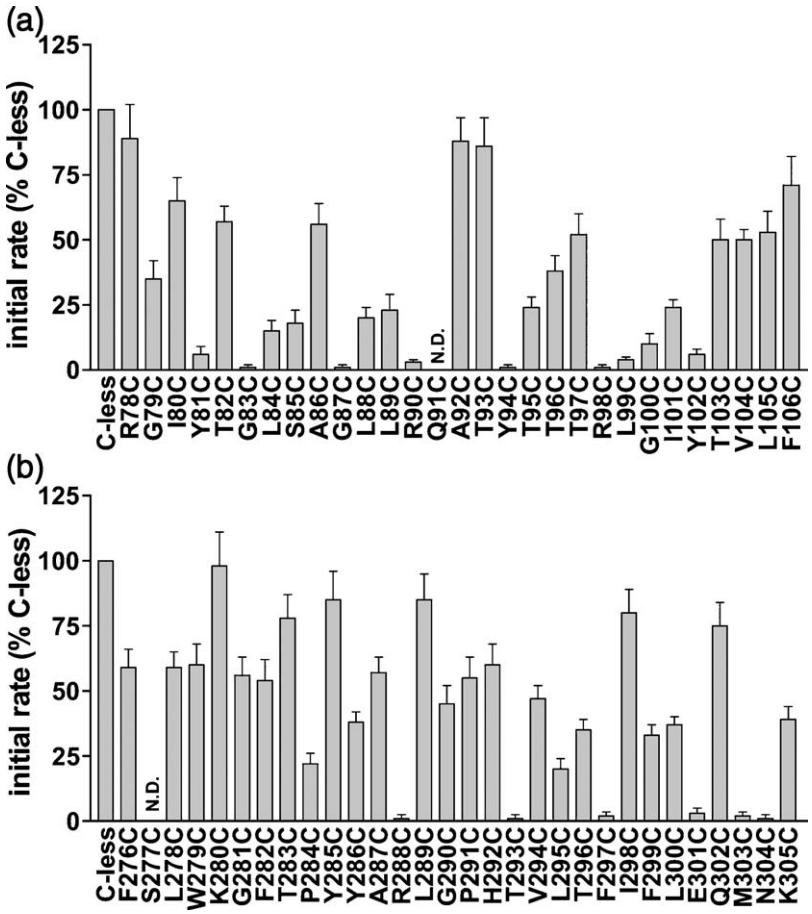

Figure 2. Initial uptake rate of 2-oxoglutarate by cysteine-less OGC and by single cysteine replacement mutant carriers for transmembrane α-helices H2 and H6. The single-letter amino acid code along the horizontal axis denotes the original residues replaced with cysteine from R78C to F106C in H2 (a) and from F276C to K305C in H6 (b). Transport was started by adding 3 mM 2-oxo[1-^{14}C]glutarate to proteoliposomes containing 20 mM 2-oxoglutarate. Initial uptake rates of oxoglutarate/oxoglutarate exchange were determined after 30 s of uptake. The data are expressed as percentage of the cysteine-less OGC value, which was on average 2491(±395) nmol min^{-1} mg^{-1} of protein (n=134). The transport activity of mutant Q91C and S277C, which were not expressed, could not be assayed (N. D., not determined). The means±S. D. of at least three independent experiments carried out in duplicate are shown.

wild-type background. All mutants had negligible transport activity compared to the wild-type OGC with the exception of the conservative substitutions T293S and F297Y (Figure 4).

Effect of sulfhydryl reagents on the transport activity of OGC mutants

Two different sulfhydryl reagents were used to probe the accessibility of cysteine residues and the effect of the cysteine modification on transport: the negatively charged MTSES and the positively charged MTSET, which are both membrane impermeable.[15–18] The residual transport activity after modification with the MTSES and MTSET reagents is shown in Figure 5 for all but the mutant proteins that lacked transport activity and for Q91C and S277C that did not express. The effect of the two reagents MTSES and MTSET was very similar with the exception of L278C and T283C, which were significantly more affected by MTSET than MTSES, and A287C, where the reverse was the case. The activity of the majority of the mutant transporters was not affected significantly by the addition of the sulfhydryl reagents. However, the mutant carriers A86C, T95C, T97C, P284C, Y285C, I298C, and F299C were inhibited by more than 90% and T96C, I101C, V294C, L295C and T296C by more than 50% by MTSES or MTSET. The results obtained with MTSES were mapped on the structural model of OGC in Figure 6 together with the available results for H4.[7]

Discussion

Here, cysteine scanning mutagenesis was employed to assess the functional importance of the amino acid residues in transmembrane α-helices H2 and H6 of the mitochondrial OGC. By using a comparative model of OGC, the results were assessed in their structural context (Figures 3 and 6). The data obtained previously for transmembrane α-helix H4 have been included, since no structure was available at the time to interpret the data.[7]

Figure 3. Effect of single cysteine replacements on the initial uptake rate of 2-oxoglutarate mapped on the structural model of OGC. The structural model of OGC is shown in cartoon (a) and surface representation (b) with a view from the cytoplasmic side (first panel) and lateral views from opposite sides (second and third panel). Single cysteine replacement carriers with 0–15%, 16–50% and 51–100% of the initial uptake rate of the cysteine-less OGC value are colored orange, yellow and green, respectively. The data are taken from Figure 2 and from Stipani *et al.*[7] The mutations that have the most severe effect on transport are also labeled with their one-letter amino acid code and their position.

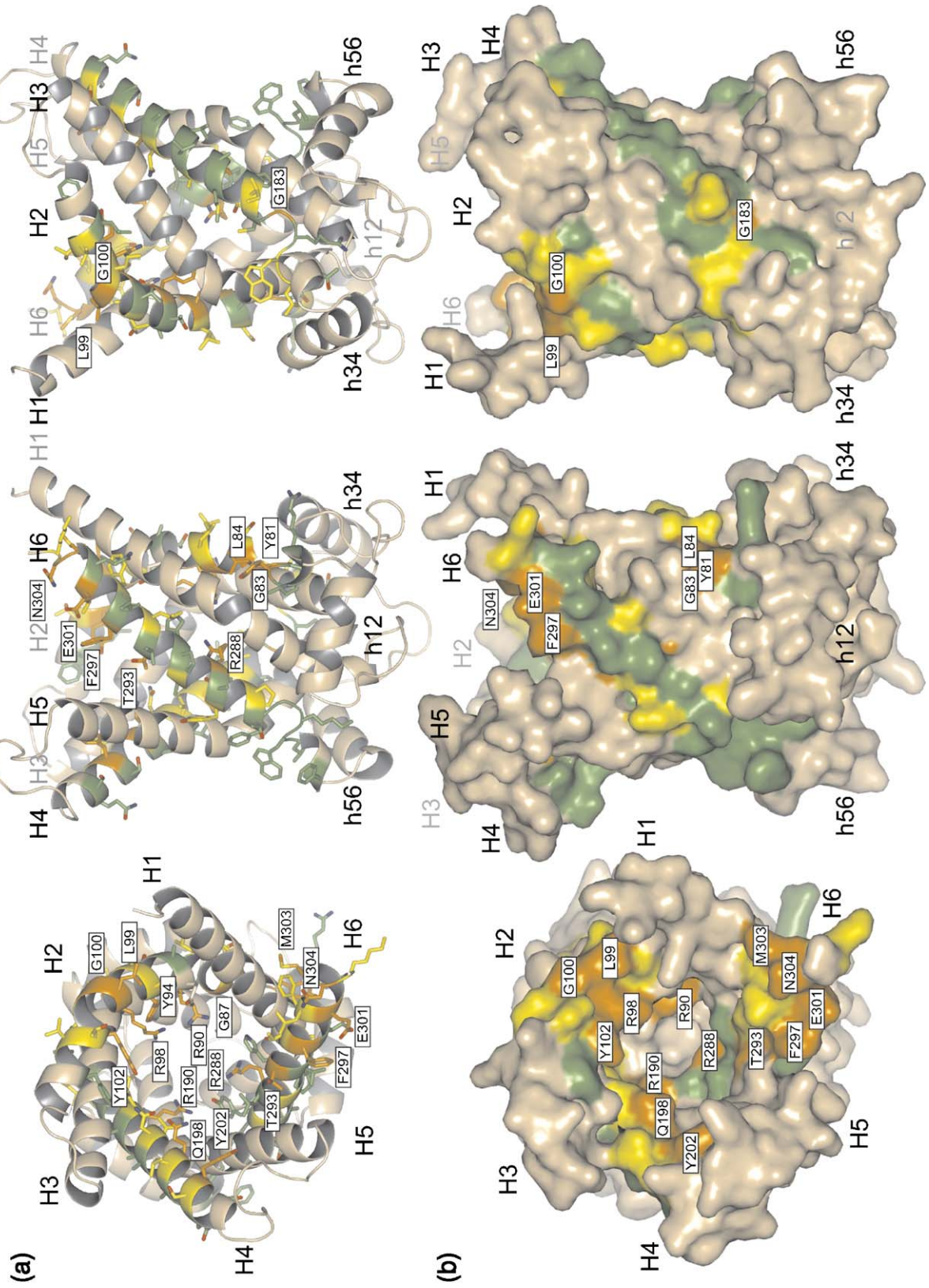

Figure 3 (*legend on previous page*)

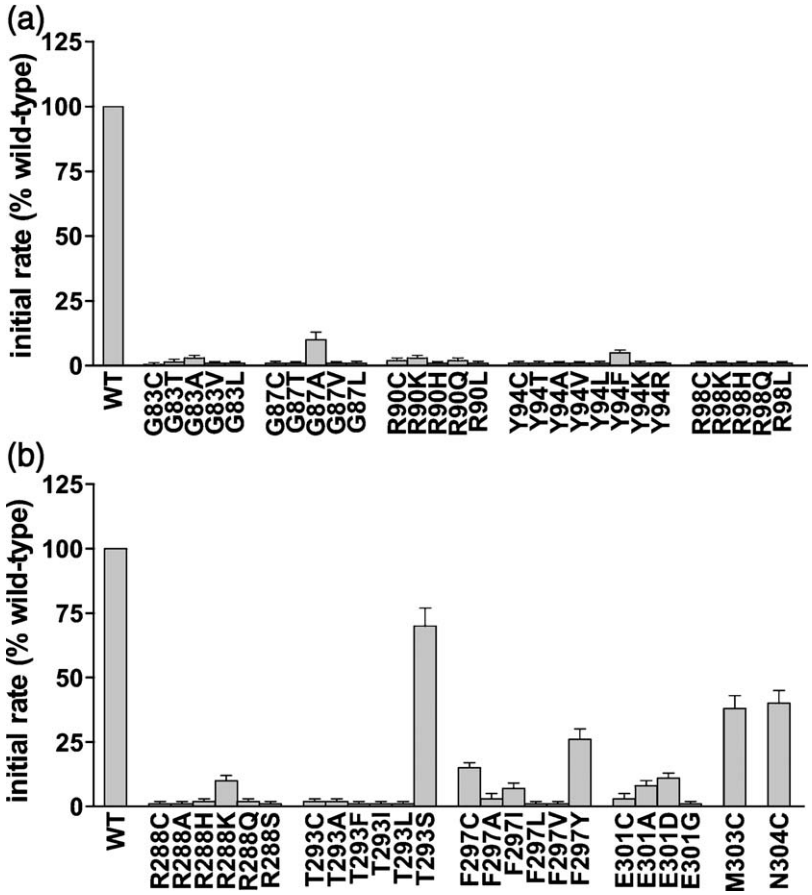

Figure 4. Transport of 2-oxoglutarate by single replacement mutants in the wild-type OGC background. The single-letter amino acid code along the horizontal axis denotes the residue replacement in H2 (a) and in H6 (b). The data are expressed as percentage of the wild-type OGC value, which was 2636(±497) nmol min^{-1} mg^{-1} of protein in 112 experiments (as initial rate).

The vast majority of cysteine mutations with a severe effect on transport activity are in the water-filled cavity of the carrier (Figure 3). Of the 23 residues of transmembrane α-helices H2, H4 and H6 predicted to line the cavity, 19 showed significant transport inhibition when mutated to cysteine, of which 12 showed total inhibition. These residues may be essential for substrate binding and the subsequent structural rearrangements that lead to the translocation of the substrate. These results are consistent with the analysis of the amino acid substitution in the OGC orthologs (Figure 1), where almost the entire cavity is fully conserved.

Of the 20 residues in the transmembrane α-helices H2, H4 and H6 that interact with the lipid bilayer, only G100C showed complete transport inactivation. Thus, the residues that interact with the acyl chains of the lipid bilayer tolerate cysteine, which is a hydrophobic substitution. Of the 26 residues that participate in inter-helical interactions, ten residues showed moderate effects and four, i.e. L99, F297, E301 and M303, showed severe effects on transport activity upon substitution. These residues may be involved in the stabilisation of the α-helical bundle and in maintaining structural integrity during conformational changes.

In the next section, the essential and important residues in the context of the comparative model and amino acid conservation will be discussed (Figure 7(a)). The most relevant residues cluster in three layers with respect to the plane of the membrane. The first cluster consists of the essential residues Y81, G83, and G183 plus residues L84, S85, A86, W181, I185, T283 and P284, where transport activity is moderately affected by the cysteine replacement and subsequent modification. These residues are in the short loops that connect the matrix and transmembrane α-helices (Figure 7(b)). They are among the few residues interacting with the membrane bilayer that do not tolerate substitution or modification and they are part of a sequence motif [YWLF]- [KR]-G-X-X-P, which is conserved in members of the mitochondrial carrier family. Mutagenesis of the residue equivalent to G183 (G174) in the yeast citrate transport protein 1 (CTP1) also affects transport activity.[18] Furthermore, the mutation G177A in the human deoxynucleotide carrier (DNC or SLC25A19) is responsible for the Amish microcephaly.[19] This conserved motif may fulfill a structural role as a helix breaker or a dynamic role as a hinge region for conformational changes during translocation.

The second cluster of important residues can be found at the carboxy-terminal end of the even-numbered transmembrane α-helices at the cytoplasmic side of the carrier (Figure 7(c)). Most sensitive to mutation and modification is the C-terminal end of H6, followed by that of H4 and H2, respectively. The conservation in the subfamily of oxoglutarate carriers follows the same order with H6 being the

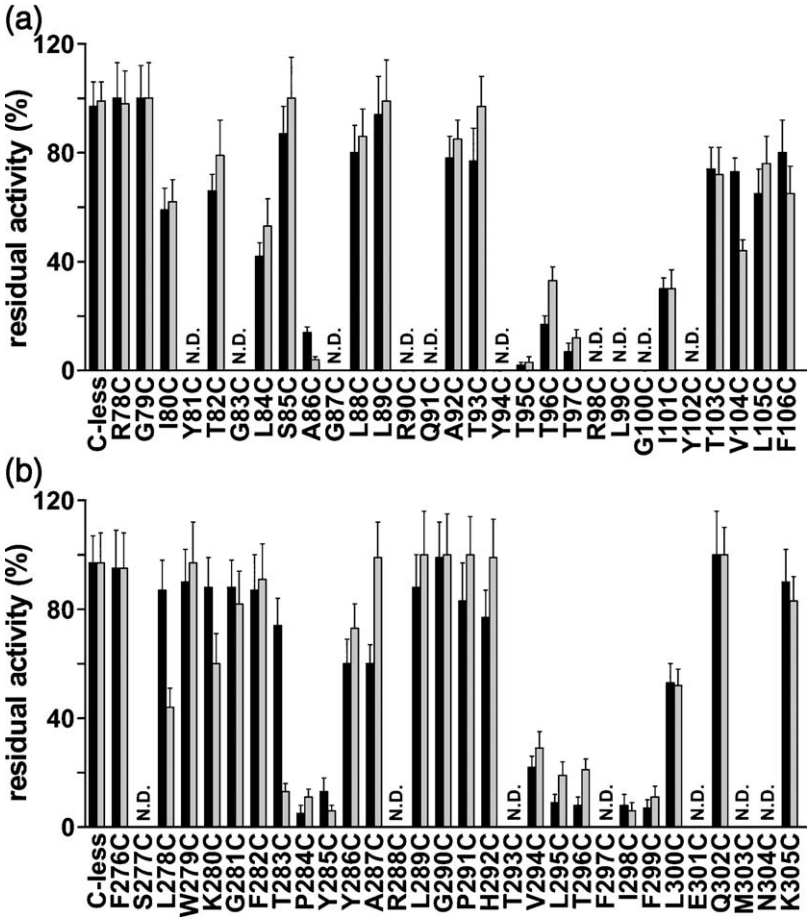

Figure 5. Effect of sulfhydryl reagents on the rate of 2-oxoglutarate uptake by cysteine-less OGC or by single cysteine replacement mutant carriers for transmembrane H2 and H6. The single-letter amino acid code along the horizontal axis denotes the original residues replaced with Cys from R78C to F106C in H2 (a) and from F276C to K305C in H6 (b). The black and grey bars represent the percentage of residual activity with MTSES or MTSET, respectively, i.e. percent of the activity in the presence of MTSES or MTSET with respect to the control value without inhibitor. Mutant carriers that were severely affected by the cysteine-replacement and Q91C and S277C, which were not expressed, could not be assayed (N.D., not determined).

best conserved (Figure 1). It is possible that H6 is conserved for the proper insertion and folding of the six-α-helical bundle during biogenesis. This region also has four important aromatic residues, Y102, Y202, F299 and F297, which could be important for inter-helical interactions.

The third cluster of important residues can be found in the cavity at the midpoint of the membrane (Figure 7(d)). The three most relevant residues are R90, R190 and R288. They are strictly conserved, they are essential for function and they are related by 3-fold pseudo-symmetry. Mutagenesis of the equivalent residues in H2 inactivates the yeast ADP/ATP carrier 2 (R96A)[20] and the rat uncoupling protein 1 (UCP1) (R84Q).[21] A mutation (G81R) in the human carnitine-acylcarnitine transporter (CACT) is associated with disease.[22] Mutation of the corresponding residue in H4 inactivates the yeast CTP1 (R181C),[18] the hamster UCP1 (R182Q)[23] and the yeast phosphate transport protein 1 (PTP1) (K179A).[24] Mutation of the equivalent residue on H6 renders the yeast AAC2 (R294A)[25] and the rat UCP1 (R276L)[21] dysfunctional. In the human ornithine carrier 1 (ORC1), the mutation R275Q in the equivalent position abolishes transport activity and is responsible for the HHH syndrome.[26,27] The residues Y285, V194, A191 and T95 are in the proximity of these essential residues in OGC and the mutant carriers are dysfunctional when their cysteine replacement is modified by sulfhydryl reagents. Thus, this area does not tolerate considerable changes to its basic structure. These data suggest that this site is critically important for the function of mitochondrial carriers. On the basis of structural and chemical similarities of substrates and the geometry of residues in the cavity a common substrate binding site has been proposed, which corresponds to the residues R90, R190 and R288 on OGC.[6] All three residues are within bonding distance of the substrate when it is docked in this site (Figure 7(d)), but the configurations of the side-chains and substrate rotamers are unknown.

If the transport activity of the single cysteine mutant carrier is affected upon modification by sulfhydryl reagents it means that the site is accessible to the label, which is water soluble. Residues in the cavity are labeled by sulfhydryl reagents, while the majority of the residues facing the lipid bilayer are not affected, implying that either these residues cannot be labeled or that the modifications have no effect on their transport activity. These results show that the transmembrane α-helices in OGC and AAC1 have the same amphipathic properties and orientation, even though they share only 18% overall sequence identity. However, a number of cysteine replacements have normal transport activity, but are sensitive to the treatment with sulfhydryl reagents. These are residues A86, T283, P284 and A287 on the matrix side and T97, V104, L295 and I298 on the

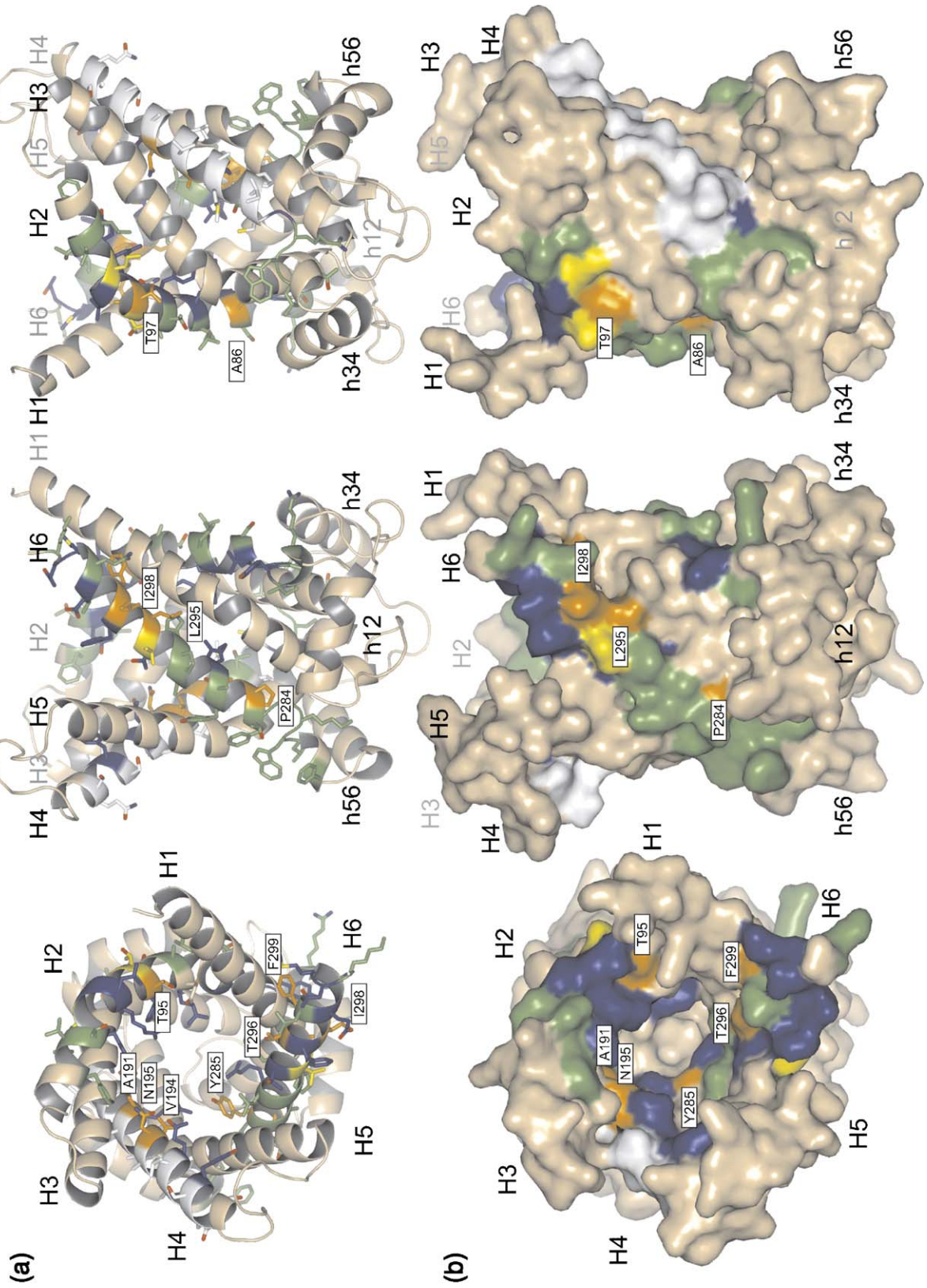

Figure 6 *(legend on opposite page)*

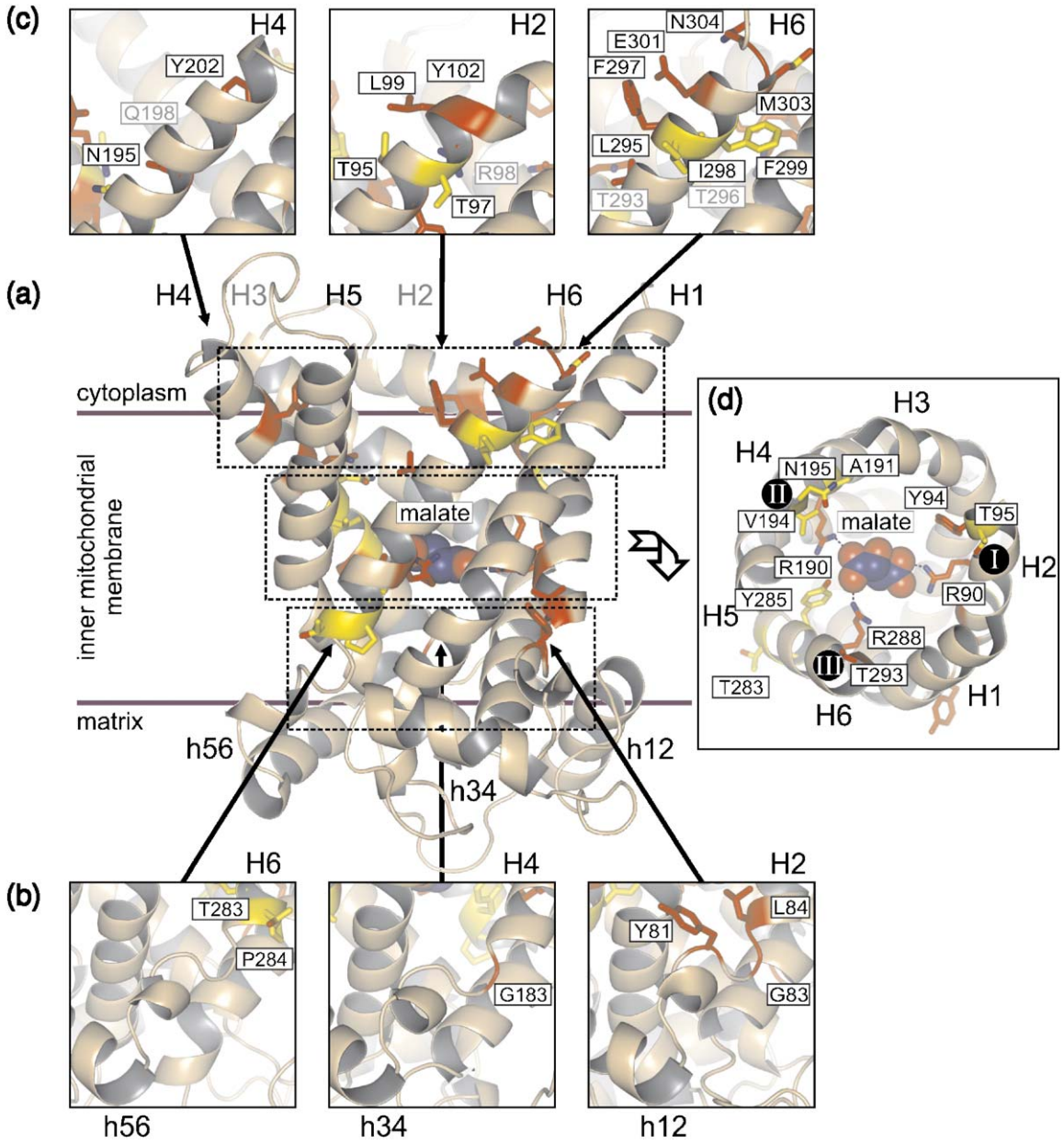

Figure 7. Overview and details of the areas most affected by the cysteine replacement and by modification by sulfhydryl reagents. (a) Cartoon representation of the structural model of OGC. Cysteine replacements that abolish transport activity are colored red, whereas cysteine replacements that abolish transport activity after labeling with sulfhydryl reagents are colored yellow. (b) Views of the amino-terminal ends and (c) the carboxy-terminal ends of α-helices H2, H4 and H6. The views are related to each other by a 120° rotation around the 3-fold pseudo-symmetry axis. (d) A view of the putative substrate binding site from the cytoplasmic side. A possible binding configuration of the substrate malate is shown in the van der Waals representation. The residues that are hidden from view are indicated by grey lettering.

cytoplasmic side of the carrier. In the model of the c-state they either face the lipid bilayer or other α-helices, and so they are not expected to be accessible to the sulfhydryl reagents, but they may be accessible when the protein is in another conformational state.

Figure 6. Effect of MTSES on the 2-oxoglutarate uptake rate mapped on the structural model of OGC. The structural model of OGC is shown in cartoon (a) and surface representation (b) with a view from the cytoplasmic side (first panel) and lateral views from opposite sides (second and third panel). The effects of MTSES on the initial uptake rate are divided into three classes: 0–15%, 16–50% and 51–100% of the rate measured in the absence of MTSES are colored orange, yellow and green, respectively. The mutations that have the most severe effect are also labeled with their one-letter amino acid code and their position. Residues that are essential for function have not been tested and are colored blue. A selected set of residues on transmembrane H4 has been tested[7] and all other ones are colored white.

Materials and Methods

Materials

2-Oxo[1-^{14}C]glutarate was purchased from Dupont De Nemours (Milan, Italy); Pipes, Triton X-114, Amberlite XAD-4 and egg yolk phospholipids (lecithin from eggs) from Fluka (Milan, Italy); *N*-dodecanoylsarcosine (sarkosyl) from Sigma (Milan, Italy); MTSES and MTSET from Fluorescent Dyes Inc. (Toronto, Canada); and Sephadex G-75 from Pharmacia (Milan, Italy). All other reagents were of analytical grade.

Construction of plasmids and site-directed mutagenesis

The cysteine-less OGC was obtained by replacing the three native cysteine residues (C184, C221 and C224) with serine using the bovine OGC cDNA fragment[28] as the template, as described.[7] Then the cysteine-less OGC cDNA was employed as a template to generate single cysteine replacement mutants. Each amino acid residue in the regions from R78 to F106 and F276 to K305, corresponding to the transmembrane α-helices H2 and H6, respectively, was replaced by cysteine in the cysteine-less OGC. Amino acid residues G83, G87, R90, Y94 and R98 in α-helix H2 and R288, T293, F297 and E301 in α-helix H6 were also mutated to various other residues in wild-type OGC. M303 and N304 were mutated in wild-type OGC only to cysteine. All mutations were introduced in the wild-type OGC cDNA or in the cysteine-less OGC cDNA by the overlap extension PCR method[29] using oligonucleotides with appropriate mutations in their sequences. The PCR products were cloned into the expression vector pMW7 and transformed into *E. coli* DH5α cells. Transformants selected on 2×TY plates containing ampicillin (100 μg/ml) were screened by direct colony PCR and by restriction digestion of the purified plasmid DNA. All mutations were verified by DNA sequencing and, except for the desired base changes, all the sequences were identical to those of wild-type or cysteine-less OGC.

Overexpression and purification of wild-type and mutant OGC

The OGC proteins were overproduced as inclusion bodies in the cytosol of *E. coli,* as described.[30,31] The inclusion bodies were purified by sucrose layer density gradient centrifugation[30] and washed at 4 °C with TE buffer (10 mM Tris–HCl (pH 8.0) and 1 mM EDTA). The inclusion bodies were washed twice with a buffer containing 10 mM Pipes (pH 7.0), 3% (w/v) Triton X-114, 1 mM EDTA and 20 mM Na_2SO_4 and then with TE buffer again. The wild-type and mutant OGC proteins were each solubilized in a buffer containing 2.5% (w/v) Sarkosyl, 1 mM EDTA and 10 mM Tris–HCl (pH 7.0). Residual material was removed by centrifugation (258,000*g* for 1 h at 4 °C).

Reconstitution of wild-type and mutant OGC proteins into liposomes and transport measurements

The recombinant proteins in Sarkosyl were reconstituted into liposomes in the presence of 20 mM 2-oxoglutarate, as described.[32] The external substrate was removed from proteoliposomes on Sephadex G-75 columns. Transport at 25 °C was started by adding 2-oxo [1-^{14}C]glutarate to eluted proteoliposomes and terminated by the addition of 20 mM pyridoxal 5′-phosphate and 16 mM bathophenanthroline.[32] In controls, the inhibitors were added with the labeled substrate at the start of the experiment. Finally, the external substrate was removed on Sephadex G-75 columns and the accumulation of labeled substrate in the proteoliposomes was measured.[32] The experimental values were corrected by subtracting control values and the transport activities were calculated by taking into account the efficiency of reconstitution, i.e. the proportion of reconstituted protein. To investigate the effect of sulfhydryl reagents on single cysteine replacement mutants, proteoliposomes were pre-incubated in the presence or absence of 5 mM MTSES or MTSET for 10 min at 25 °C. After removal of unbound reagent by Sephadex G-75 chromatography, transport was initiated by adding 0.3 mM 2-oxo[1-^{14}C]glutarate and terminated after 30 s.

Additional experimental methods

SDS-PAGE was performed essentially as described.[33] The amount of recombinant protein was estimated from Coomassie blue-stained SDS–PAGE gels with the Bio-Rad GS-700 Imaging Densitometer (Bio-Rad Laboratories, San Francisco, USA) using carbonic anhydrase as the standard. The levels of mutant OGC protein expression were evaluated by Western blotting with a rabbit antiserum raised against OGC protein isolated from bovine heart mitochondria, as described.[34] The extent of incorporation of the recombinant protein into liposomes was determined as described by Phelps *et al.*,[8] except that protein concentration was determined by laser densitometry of stained SDS–gels after extraction of lipid by organic solvents.[35]

Comparative model of the bovine oxoglutarate carrier

The structure of the bovine AAC1 contains the tightly bound inhibitor carboxy-atractyloside. The 3-fold pseudo-symmetry is structurally conserved in the binding site, which shows that the Cα positions in this area are not significantly altered by the binding. A structural model of the bovine OGC was built based upon the structure of the bovine AAC1 by using the computer application MODELLER.[36] A critical determinant in the accuracy of comparative modeling is the quality of the pair-wise sequence alignment between the OGC target and AAC1 template sequences. As the similarity between the OGC and AAC1 proteins is lower than normally considered appropriate for comparative modeling, a multiple sequence alignment strategy was used to generate pair-wise alignments. AAC1 and OGC were added to sequences from the mitochondrial carrier family of yeast. A multiple sequence alignment was generated by CLUSTAL W[37] with the secondary structure of AAC1 used to weight the gap penalties so that there was preferential placement of insertions and deletions in loops. The multiple sequence alignment highlighted residues that were strongly conserved across the family members and they served as anchor points in the alignment, which improved the quality of the pair-wise alignment between AAC1 and OGC.[6] There is very little ambiguity in the alignments because of the threefold repeats, signature motifs and other highly conserved amino acid residues. The transmembrane α-helices are also strongly amphipathic, with one face of each α-helix interacting with the lipid bilayer

and the other facing the water-filled cavity. These special properties provide additional constraints. The OGC sequence was trimmed at its N and C termini so that it did not extend beyond the bovine AAC1 sequence for which there was no structure available. Where the loops of the OGC were shorter than the corresponding loops of the bovine AAC1, the sequence gap was placed such that the distance between the gap ends in the initial starting structure was minimized. During the modeling process, the C^{α} backbone of the OGC target was restrained to the backbone of the AAC1 template structure. Distance constraints were placed between the residues of the salt bridges in the OGC target. A slow molecular dynamics simulation with an annealing procedure was repeated to generate 100 optimized OGC structures under these restraints and constraints. The structural properties of the OGC models with the best energy function were evaluated using the application MolProbity.[38] Final models were examined in PyMOL, and where side-chain packing led to gaps between transmembrane α-helices alternative side-chain rotamers were evaluated.

Analysis of amino acid substitution

The OGC orthologs were identified in the following organisms: *Anopheles gambiae*, *Drosophila melanogaster*, *D. pseudoobscura*, *Caenorhabditis elegans*, *C. briggsae*, *Bos taurus*, *Homo sapiens*, *Oryza sativa*, *Pan troglodytes*, *Pongo pygmaeus*, *Mus musculus*, *Rattus norvegicus*, *Danio rerio*, *Xenopus laevis* and *Tetraodon nigroviridis*. The sequences were obtained from UniProt†. The amino acid sequences of the orthologs were aligned with CLUSTAL W and the number of amino acid substitutions per position was determined.

Acknowledgements

This work was supported by grants from MIUR, the Center of Excellence in Genomics (CEGBA), MIUR L. 488/92 (cluster 03), EC contract LSHM-CT-2004-503116 and the UK Medical Research Council.

References

1. Palmieri, F., Quagliariello, E. & Klingenberg, M. (1972). Kinetics and specificity of the oxoglutarate carrier in rat-liver mitochondria. *Eur. J. Biochem.* **29**, 408–416.
2. Palmieri, F. (2004). The mitochondrial transporter family (SLC25): physiological and pathological implications. In "The ABC of solute carriers". *Pflugers Arch. - Eur. J. Physiol.* **447**, 689–709.
3. Pebay-Peyroula, E., Dahout-Gonzalez, C., Kahn, R., Trezeguet, V., Lauquin, G. J. & Brandolin, G. (2003). Structure of mitochondrial ADP/ATP carrier in complex with carboxyatractyloside. *Nature*, **426**, 39–44.
4. Kunji, E. R. & Harding, M. (2003). Projection structure of the atractyloside-inhibited mitochondrial ADP/ATP carrier of Saccharomyces cerevisiae. *J. Biol. Chem.* **278**, 36985–36988.
5. Nelson, D. R., Felix, C. M. & Swanson, J. M. (1998). Highly conserved charge-pair networks in the mitochondrial carrier family. *J. Mol. Biol.* **277**, 285–308.
6. Robinson, A. J. & Kunji, E. R. (2006). Mitochondrial carriers in the cytoplasmic state have a common substrate binding site. *Proc. Natl Acad. Sci. USA*, **103**, 2617–2622.
7. Stipani, V., Cappello, A. R., Daddabbo, L., Natuzzi, D., Miniero, D. V., Stipani, I. & Palmieri, F. (2001). The mitochondrial oxoglutarate carrier: cysteine-scanning mutagenesis of transmembrane domain IV and sensitivity of cys mutants to sulphydryl reagents. *Biochemistry*, **40**, 15805–15810.
8. Phelps, A., Briggs, C., Mincone, L. & Wohlrab, H. (1996). Mitochondrial phosphate transport protein. replacements of glutamic, aspartic, and histidine residues affect transport and protein conformation and point to a coupled proton transport path. *Biochemistry*, **35**, 10757–10762.
9. Fiermonte, G., Palmieri, L., Dolce, V., Lasorsa, F. M., Palmieri, F., Runswick, M. J. & Walker, J. E. (1998). The sequence, bacterial expression and functional reconstitution of the rat mitochondrial dicarboxylate transporter cloned via distant homologs in yeast and *Caenorhabditis elegans*. *J. Biol. Chem.* **273**, 24754–24759.
10. Briggs, C., Mincone, L. & Wohlrab, H. (1999). Replacements of basic and hydroxyl amino acids identify structurally and functionally sensitive regions of the mitochondrial phosphate transport protein. *Biochemistry*, **38**, 5096–5102.
11. Dolce, V., Fiermonte, G., Runswick, M. J., Palmieri, F. & Walker, J. E. (2001). The human mitochondrial deoxynucleotide carrier and its role in toxicity of nucleoside antivirals. *Proc. Natl Acad. Sci. USA*, **98**, 2284–2288.
12. Palmieri, L., Pardo, B., Lasorsa, F. M., del Arco, A., Kobayashi, K., Iijima, M. *et al.* (2001). Citrin and aralar1 are Ca^{2+}-stimulated aspartate/glutamate transporters in mitochondria. *EMBO J.* **20**, 5060–5069.
13. Marobbio, C. M. T., Agrimi, G., Lasorsa, F. M. & Palmieri, F. (2003). Identification and functional reconstitution of yeast mitochondrial carrier for S-adenosylmethionine. *EMBO J.* **22**, 5975–5982.
14. Fiermonte, G., De Leonardis, F., Todisco, S., Palmieri, L., Lasorsa, F. M. & Palmieri, F. (2004). Identification of the mitochondrial ATP-Mg/Pi transporter: bacterial expression, reconstitution, functional characterization and tissue distribution. *J. Biol. Chem.* **279**, 30722–30730.
15. Akabas, M. H., Stauffer, D. A., Xu, M. & Karlin, A. (1992). Acetylcholine receptor channel structure probed in cysteine-substitution mutants. *Science*, **258**, 307–310.
16. van Iwaarden, P. R., Driessen, A. J. & Konings, W. N. (1992). What we can learn from the effects of thiol reagents on transport proteins. *Biochim. Biophys. Acta*, **1113**, 161–170.
17. Yan, R. T. & Maloney, P. C. (1993). Identification of a residue in the translocation pathway of a membrane carrier. *Cell*, **75**, 37–44.
18. Kaplan, R. S., Mayor, J. A., Brauer, D., Kotaria, R., Walters, D. E. & Dean, A. M. (2000). The yeast mitochondrial citrate transport protein. Probing the secondary structure of transmembrane domain iv and identification of residues that likely comprise a portion of the citrate translocation pathway. *J. Biol. Chem.* **275**, 12009–12016.
19. Rosenberg, M. J., Agarwala, R., Bouffard, G., Davis, J., Fiermonte, G., Hilliard, M. S. *et al.* (2002). Mutant

† http://www.ebi.uniprot.org

deoxynucleotide carrier is associated with congenital microcephaly. *Nature Genet.* **32**, 175–179.
20. Muller, V., Heidkamper, D., Nelson, D. R. & Klingenberg, M. (1997). Mutagenesis of some positive and negative residues occurring in repeat triad residues in the ADP/ATP carrier from yeast. *Biochemistry*, **36**, 16008–16018.
21. Modriansky, M., Murdza-Inglis, D. L., Patel, H. V., Freeman, K. B. & Garlid, K. D. (1997). Identification by site-directed mutagenesis of three arginines in uncoupling protein that are essential for nucleotide binding and inhibition. *J. Biol. Chem.* **272**, 24759–24762.
22. IJlst, L., van Roermund, C. W., Iacobazzi, V., Oostheim, W., Ruiter, J. P., Williams, J. C. *et al.* (2001). Functional analysis of mutant human carnitine acylcarnitine translocases in yeast. *Biochem. Biophys. Res. Commun.* **280**, 700–706.
23. Klingenberg, M. & Echtay, K. S. (2001). Uncoupling proteins: the issues from a biochemist point of view. *Biochim. Biophys. Acta*, **1504**, 128–143.
24. Wohlrab, H., Annese, V. & Haefele, A. (2002). Single replacement constructs of all hydroxyl, basic, and acidic amino acids identify new function and structure-sensitive regions of the mitochondrial phosphate transport protein. *Biochemistry*, **41**, 3254–3261.
25. Heidkamper, D., Muller, V., Nelson, D. R. & Klingenberg, M. (1996). Probing the role of positive residues in the ADP/ATP carrier from yeast. The effect of six arginine mutations on transport and the four ATP versus ADP exchange modes. *Biochemistry*, **35**, 16144–16152.
26. Salvi, S., Dionisi-Vici, C., Bertini, E., Verardo, M. & Santorelli, F. M. (2001). Seven novel mutations in the ORNT1 gene (SLC25A15) in patients with hyperornithinemia, hyperammonemia, and homocitrullinuria syndrome. *Hum. Mutat.* **18**, 460.
27. Fiermonte, G., Dolce, V., David, L., Santorelli, F. M., Dionisi-Vici, C., Palmieri, F. & Walker, J. E. (2003). The mitochondrial ornithine transporter: bacterial expression, reconstitution, functional characterization, and tissue distribution of two human isoforms. *J. Biol. Chem.* **278**, 32778–32783.
28. Runswick, M. J., Walker, J. E., Bisaccia, F., Iacobazzi, V. & Palmieri, F. (1990). Sequence of the bovine 2-oxoglutarate/malate carrier protein: structural relationship to other mitochondrial transport proteins. *Biochemistry*, **29**, 11033–11040.
29. Ho, S. N., Hunt, H. D., Horton, R. M., Pullen, J. K. & Pease, L. R. (1989). Site-directed mutagenesis by overlap extension using the polymerase chain reaction. *Gene*, **77**, 51–59.
30. Fiermonte, G., Walker, J. E. & Palmieri, F. (1993). Abundant bacterial expression and reconstitution of an intrinsic membrane transport protein from bovine mitochondria. *Biochem. J.* **294**, 293–299.
31. Marobbio, C. M. T., Vozza, A., Harding, M., Bisaccia, F., Palmieri, F. & Walker, J. E. (2002). Identification and reconstitution of the yeast mitochondrial transporter for thiamine pyrophosphate. *EMBO J.* **21**, 5653–5661.
32. Palmieri, F., Indiveri, C., Bisaccia, F. & Iacobazzi, V. (1995). Mitochondrial metabolite carrier proteins: purification, reconstitution and transport studies. *Methods Enzymol.* **260**, 349–369.
33. Laemmli, U. K. (1970). Cleavage of structural proteins during the assembly of the head of bacteriophage T4. *Nature*, **227**, 680–685.
34. Bisaccia, F., Capobianco, L., Brandolin, G. & Palmieri, F. (1994). Transmembrane topography of the mitochondrial oxoglutarate carrier assessed by peptide-specific antibodies and enzymatic cleavage. *Biochemistry*, **33**, 3705–3713.
35. Fiermonte, G., Dolce, V. & Palmieri, F. (1998). Expression in *Escherichia coli*, functional characterization, and tissue distribution of isoforms A and B of the phosphate carrier from bovine mitochondria. *J. Biol. Chem.* **273**, 22782–22787.
36. Sali, A. & Blundell, T. L. (1993). Comparative protein modelling by satisfaction of spatial restraints. *J. Mol. Biol.* **234**, 779–815.
37. Thompson, J. D., Higgins, D. G. & Gibson, T. J. (1994). CLUSTAL W: improving the sensitivity of progressive multiple sequence alignment through sequence weighting, position-specific gap penalties and weight matrix choice. *Nucl. Acids Res.* **22**, 4673–4678.
38. Lovell, S. C., Davis, I. W., Arendall, W. B., III, de Bakker, P. I., Word, J. M., Prisant, M. G. *et al.* (2003). Structure validation by Calpha geometry: phi,psi and Cbeta deviation. *Proteins*, **50**, 437–450.

Edited by I. B. Holland

(Received 30 June 2006; received in revised form 2 August 2006; accepted 14 August 2006)
Available online 22 August 2006